# Chromatic transition of π-conjugated polydiacetylene and the subsequent aggregation phenomena

Hidetoshi Oikawa*, Tatsumi Korenaga, Shuji Okada, Hachiro Nakanishi

*Institute for Chemical Reaction Science, Tohoku University, Katahira 2-1-1 Aoba-ku, Sendai 980-8577, Japan*

## Abstract

Static and dynamic light scattering from π-conjugated poly(4BCMU) in toluene solutions were measured at 353 K (yellow phase) and 323 K (red phase) to evaluate the hydrodynamic radius $R_h$ and the fractal dimension $D$. It was suggested that poly(4BCMU) may exist not as an isolated worm-like chain but as a weakly interacted cluster-like domain in the yellow phase. The domain was considered to be elaborated by inter-molecular hydrogen bondings formed newly through a thermal break of intra-molecular hydrogen bondings between side chains along a main chain. On the other hand, the increases in $R_h$ and $D$ have revealed that poly(4BCMU) chains aggregated gradually in the red phase, after taking a single extended rod-like conformation. The subsequent aggregation seemed to be promoted not only by lowering a solvent quality but also by increasing the effective concentration, accompanied by the conformational transition. © 1999 Elsevier Science Ltd. All rights reserved.

## 1. Introduction

Polydiacetylene (PDA), $(=CR-C≡C-CR=)_n$, which is commonly synthesized by solid-state polymerizing diacetylene monomer in a single crystal state [1], was studied extensively on crystal structure [2], the electronic [3], mechanical [4], optical [5], and conformational properties [6] in solid states of crystals and thin films [7,8] and is of interest in connection with long quasi-one-dimensional π-conjugated structure [9]. Especially, PDA was paid much attention as one of the most promising organic non-linear optical materials, which may indicate high third-order optical susceptibility [10–12], large optical non-linearity, and high photoconductivity [13,14]. PDA was the subject of several reviews and books [9,15–17].

Most of PDA are infusible and insoluble even in an exotic solvent, because of their rotation-restricted stiff backbone [1,18], except for some PDA such as poly(nBCMU), which side chain is customarily known to be $R = -(CH_2)_nO-CONHCH_2COO(CH_2)_3CH_3$ with $n = 3$ and 4. These soluble PDA's indicate peculiar colour changes in their solutions [19–23], which reflects essentially the colour changes in a crystal state. For example, poly(4BCMU), poly[5,7-dodeca-diynylenebis(N-butoxycarbonlymethylcarbonate)], in toluene solution is usually red at room temperature, and turns yellow either by raising temperature or by adding chloroform as a good solvent [20,21]. The colour change properties of PDA are expected as a sensor or an indicator [24–26] to measure temperature, pressure, radiation dosage, gas exposure, pH and humidity.

The chromatic transition of a soluble PDA is said to be induced primarily by a conformational transition, which is correlated closely with the effective length of π-conjugation along a main chain [27]. Nevertheless, this phenomenon is not so simple but dependent on many experimental factors: solvent quality, temperature, pressure, concentration and time [20]. The mechanisms of the chromatic transition already proposed were classified mainly into two groups: one is an intra-molecular rod-to-coil conformational transition in a single PDA chain [28–30]; the other responsible for an inter-molecular effect, which often attends a formation of aggregated rod-like PDA chains [31–33]. In practice, some models concerning PDA conformation in a coiled state were proposed: (ribbon) worm-like chain model [31,32], discrete random-flight chain model (or platelet model with Kuhn-chain) [31,32], and *trans*-to-*cis* isomeric configuration model [34]. On the other hand, two passes were postulated for an aggregation process: the consequential inter-molecular aggregation by the already extended rod-like PDA chain

* Corresponding author. Tel.: + 81-22-217-5644; fax: + 81-22-217-5645.

*E-mail address:* hoikawa@icrs.tohoku.ac.jp (H. Oikawa)

Table 1
Hydrodynamic radius $R_h$ and fractal dimension $D$ of Poly(4BCMU)-toluene systems evaluated at 353 K (yellow phase) and 323 K (red phase)

| Temperature (elapsed time) | Non-surfactant | | Addition of surfactant | |
|---|---|---|---|---|
| | $R_h$/nm | $D$ | $R_h$/nm | $D$ |
| 353 K | 1600 | | 210(TX)[a], 250(OG)[b] | |
| 323 K (0 h) | 88 | 1.0 | | 1.1(TX)[a], 1.5(OG)[b] |
| 323 K (12 h) | 230 | 2.3 | 250(TX)[a], 230(OG)[b] | 2.7(TX)[a], 2.3(OG)[b] |

[a] TX indicates Triton X-100 surfactant. Refer to Section 2.
[b] OG denotes OG surfactant. Refer to Section 2.

and the subsequent extension to rod-like conformation by the occurrence of aggregation [20]. At the present time, as the most probable explanation, it is described by Chu et al. that PDA chain is a worm-like coil in a good solvent, rod aggregates formed in a poor solvent, and that PDA may become more extended in rod aggregates [20].

In the present study, static and dynamic light scattering (SLS and DLS) measurements for poly(4BCMU) in toluene solutions were performed to evaluate the hydrodynamic radius and the fractal dimension [35,36]. To clarify these confused arguments mentioned earlier, the following experimental items were particularly investigated with attention: (1) the effect of conformational transition of PDA chains on crossover concentration; (2) to realize kinetically slow aggregation in a moderate state of poor solvent; and (3) the influence of added surfactants.

## 2. Experimental section

### 2.1. Materials and preparations

The so-called 4BCMU (butoxy carbonyl methyl urethane) diacetylene monomer, $RC{\equiv}C{-}C{\equiv}CR$, used in the present study was synthesized and crystallized [27]. The functional group $R$ in 4BCMU has already been
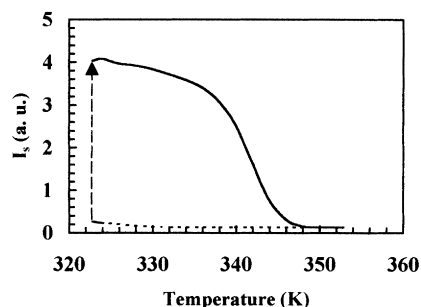


Fig. 1. Variations of scattered light intensity $I_s$ from poly(4BCMU)-toluene solution with thermal hysteresis: cooling process (dotted line), the process maintained at 323 K (broken line), and heating process (full line). The volume fraction of polymer $\phi_2$ was $3.4 \times 10^{-5}$ in toluene solution. The hot toluene solution at 353 K was cooled up to 323 K, and held at this temperature. After ca. 12 h, $I_s$ reached the steady-state, and was then heated up to 353 K again. The cooling and heating rates were 0.3 K min$^{-1}$. The scattering angle $\theta$ was 90°.

represented in Section 1. The single crystals of 4BCMU monomers were solid-state polymerized by γ-ray irradiation ($^{60}$Co − source: 100 Mrad) at room temperature. For purification the resulting poly(4BCMU) was dissolved in chloroform (CHCl$_3$) (ca. 0.5 g L$^{-1}$) at room temperature, being said not to associate and/or aggregate in diluted CHCl$_3$ solution [37], reprecipitated in a large excess of $n$-hexane, and then dried in vacuo. The weight-average molecular weight $M_w$ was $1.8 \times 10^6$, which was determined by means of a low-angle laser light scattering instrument (Tosoh Corp.: LS-8). The distribution of molecular weight $M_w/M_n$ was relatively broad and roughly four to five, by using GPC (Shimadzu: LC-8A Series), which had been calibrated with a mono-dispersed polystyrene (Tosoh Corp., TSK Standard Polystyrene Series).

A given amount of purified poly(4BCMU) was dissolved completely in toluene at 353 K. The solvent used was an analytical grade reagent and employed without further purification. Afterwards, the toluene solution was passed immediately through a 0.2 μm membrane filter (Advantec Toyo Inc., 25HP020AN) to remove dust for light scattering measurements. In some cases, two kinds of non-ionic surfactants were added: Triton X-100, [polyoxyethlenegly-col (10) $p$-$t$-octylphenyl ether]; OG, [$n$-octyl-β-D-gluco-side]. The amount of surfactants added was about ten times as much as monomer concentration. All operations for preparations were carried out in a clean bench to avoid dust in the air.

### 2.2. UV spectrum and light scattering measurements

The color of poly(4BCMU)-toluene solution were measured with a UV-VIS spectrometer (Shimadzu: UV-240) with a thermostat. The SLS and DLS (homodyne spectroscopy) [36] apparatus used was DLS-7000 (Otsuka Electronics Co. Ltd.), which was equipped with He-Ne laser source (10 mW, λ = 632.8 nm) and a thermostat.

## 3. Results

All the experimental results obtained were summarized in Table 1. Fig. 1 exhibits the variations of scattered light intensity $I_s$ from poly(4BCMU)-toluene solution with thermal hysteresis at scattering angle θ = 90°. The volume
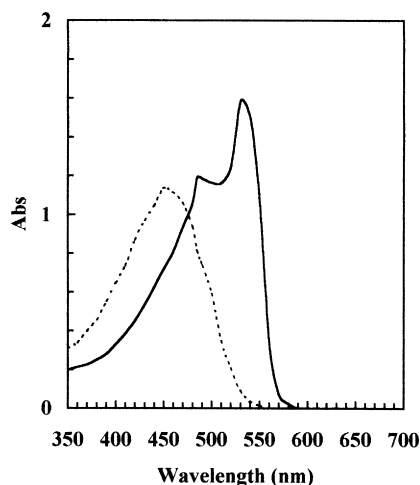
Fig. 2. Visible absorption spectra at 353 K (yellow phase) and at $t_{323\,K} = 12$ (red phase). $t_{323\,K}$ denotes the elapse of time (in an hour unit) at 323 K. The steady-state in the red phase was established at $t_{323\,K} = 12$.

fraction of polymer $\phi_2$ was $3.4 \times 10^{-5}$ in toluene solution. The toluene solution stored in a dark place at room temperature was heated once at 353 K for a given time so that $I_s$ could become steady-state. The hot toluene solution at 353 K started to be cooled at the cooling rate of 0.3 K min$^{-1}$ up to 323 K, and was maintained at that temperature for about half a day. $I_s$ increased slightly on the cooling process, and became high gradually with the elapse of time at 323 K. After ca. 12 h, $I_s$ reached the steady-state. No aggregation and precipitate, however, were observed macroscopically with the eye, and the toluene solution was still optically clear at that time. Afterwards, the toluene solution was heated again at the same rate up to 353 K. $I_s$ decreased up to the same level as the initial $I_s$. Hereafter, $t_{323\,K}$ denotes the elapse of time (in an hour unit) at 323 K.

Fig. 2 shows the visible absorption spectra at 353 K and at $t_{323\,K} = 12$. Thus, the spectrum measured at 323 K was the one at the steady-state. The wavelengths at maximum absorption peaks $\lambda_{max}$ were 456 nm (yellow phase) at 353 K and 535 nm (red phase) at $t_{323\,K} = 12$, respectively. These two spectra were essentially similar to those described elsewhere [28,38].
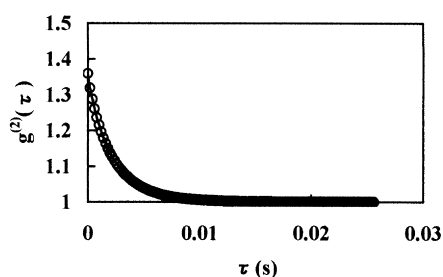


Fig. 3. Normalized second-order intensity autocorrelation function (ACF) of the photocurrent $g^{(2)}(\tau)$ of poly(4BCMU)-toluene solution measured at 353 K (yellow phase). The full line represents the best fit by Eqs. (1) and (2). $\tau$ is the correlation time. The scattering angle $\theta$ was 90°.

### 3.1. Yellow phase at 353 K

The normalized second-order intensity autocorrelation function (ACF) of the photocurrent $g^{(2)}(\tau)$ measured in the yellow phase is shown in Fig. 3, and $\tau$ is the correlation time. Fig. 4 indicates the dependence of decay constant $\Gamma$ on the scattering vector $q^{36}$. The value of $\Gamma q^{-2}$ on the ordinate corresponds to an apparent translational diffusion constant $D_{app}$ at a given $q^{36}$. In the present study, $\Gamma$ was evaluated from the Siegert relation [Eq. (1)] [35,36] by fitting the Kohlrausch–Williams–Watts (KWW) equation [Eq. (2)] [39,40] to the measured ACF:

$$g^{(2)}(\tau) = 1 + \beta|g^{(1)}(\tau)|^2 \tag{1}$$

$$g^{(1)}(\tau) = \exp\{-(\Gamma\tau)^\gamma\} \quad 0 < \gamma \leq 1 \tag{2}$$

where, $g^{(1)}(\tau)$ is the normalized first-order intensity ACF of the photoelectric field, $\beta$ is the factor depending on the coherence of the detector, and $\gamma$ is the exponent, which is correlated to the distribution of $\Gamma$. The KWW equation [Eq. (2)] is usually available for a broad distribution of $\Gamma$, for example, in the case of a wide distribution of molecular weight. However, on the contrary, the exponent $\gamma$ was about 0.90 in any scattering angles $\theta$ in the yellow phase, in spite of $M_w/M_n = 4$–5 as described in Section 2. It follows that the ACF measured approximately decayed single-exponentially. In addition, the up-turn phenomenon of $\Gamma q^{-2}$ was observed at low $q$-region. The ACF measured at the low $q$-region seems to be influenced by a stray light on the wall of the cell [41], owing to remarkably low $I_s$ in the yellow phase as shown in Fig. 1. So, as represented by the broken line drawn in Fig. 4, $D_{app}$ was averaged by neglecting the experimental data at the low $q$-region. The corresponding hydrodynamic radius $R_h$ was calculated to be 1600 nm, in accordance with the following Einstein–Stokes relation [42]:

$$R_h = k_B T/6\pi\eta_0 D_{app} \tag{3}$$

where, $k_B$, T, and $\eta_0$ are Boltzmann's constant, the absolute temperature, and the viscosity of the medium, respectively.

The relationship between $\phi_2 I_s^{-1}$ and $\phi_2$ is plotted in Fig. 5 (so-called Debye-type plot [35]). The ordinate is an arbitrary unit, since it was difficult experimentally to measure accurately an increment of refractive index with concentration $\partial n/\partial c$ at high temperature such as 353 K. However, all the slopes were confirmed to be negative at any $\theta$.

As described later in Section 4, the surfactants such as Triton X-100 and OG were added to investigate further the dissolution situation of poly(4BCMU) in the yellow phase. In a word, the values of $R_h$ in the yellow phase were compared before and after adding the surfactants. Figs. 6 and 7 represent the decay curve of $g^{(2)}(\tau)$ in the presence of Triton X-100, and the corresponding plots of $\Gamma q^{-2}$ versus $q^2$. The obtained exponent $\gamma$ was a little low at 0.80, compared with that in Fig. 4. The value of $R_h$ was 210 nm
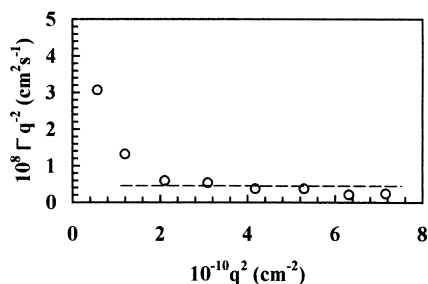
Fig. 4. Relationship between $\Gamma q^{-2}$ and $q^2$ in the yellow phase. $\Gamma$ is a decay constant, which was determined by fitting the KWW equation [Eq. (2)] to the measured ACF, and $q$ is a scattering vector. The broken line represents $\Gamma q^{-2}$ averaged by neglecting the experimental data at a low $q$-region.

in this case. Similarly, $R_h$ was determined to be 250 nm, when OG was added.

### 3.2. Red phase at 323 K

The decay curve of $g^{(2)}(\tau)$ at $t_{323\ K} = 12$ in the red phase is shown in Fig. 8, and Fig. 9 indicates the dependence of $\Gamma q^{-2}$ on $q^2$ at $t_{323\ K} = 12$, which yielded a $R_h$ of 230 nm in a similar manner as shown earlier. The exponent $\gamma$ in the KWW equation [Eq. (2)] was 0.88 in Fig. 8.

As shown in Fig. 10, the time-evolution of $I_s$ was obtained as a function of $q$ at various $t_{323\ K}$, and the slope $\alpha$ in the log–log plots corresponds to fractal dimension $D$ as the following expression [43,44]:

$$I_s \sim q^{-\alpha} \tag{4}$$

Here, (i) $D = \alpha$ at $\alpha \leq 3$ for mass fractals; (ii) $D = 2d_E - \alpha$ at $\alpha > 3$ for surface fractals. $d_E$ is the Euclidean dimension. The present experimental results shown in Fig. 10 relate to case (i).

The changes of $R_h$, $D$, $\lambda_{max}$, and absorbance at $\lambda_{max}$, Abs($\lambda_{max}$), with $t_{323\ K}$ are displayed in Fig. 11(a), (b) and
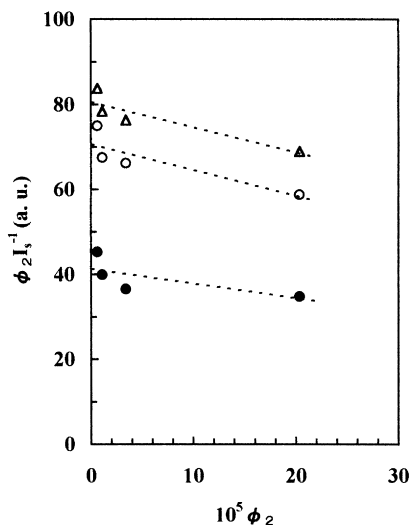


Fig. 5. Dependence of $I_s \phi_2^{-1}$ on $\phi_2$ (Debye-type plot) in the yellow phase. Scattering angles $\theta$ were 30°(●), 60°(○), and 90°(△).
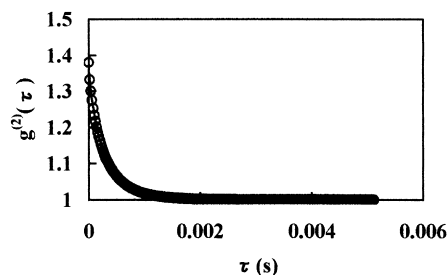


Fig. 6. Decay curve of $g^{(2)}(\tau)$ measured at 353 K (yellow phase) in the presence of Triton X-100. The full line displays the best fit by Eqs. (1) and (2). $\theta$ was 90°.

(c), respectively. Over the period of about 12 h at 323 K, $R_h$ increased exponentially from 88 nm to 230 nm, and the $D$ values were changed from ca. 1.0 to 2.3. After more than 12 hours, not only $I_s$ but also $R_h$ and $D$ have become almost constant within the experimental error. On the other hand, $\lambda_{max}$ and Abs($\lambda_{max}$) were reached approximately to the steady-state within about 2 h. However, the shift of $\lambda_{max}$ during the initial 2 h at 323 K was approximately 3 nm, less than 3%, compared with the shifted value in $\lambda_{max}$ for yellow-to-red colour change.

As summarized in Table 1, the value of $R_h$ at $t_{323\ K} = 12$ was estimated to be 250 nm in the presence of Triton X-100 (see also Fig. 12), whereas $R_h$ was 230 nm in case of OG. It was also found that the added surfactants affected neither $\lambda_{max}$ and Abs($\lambda_{max}$) nor $D$, and that did not prevent the entire aggregation process in the red phase.

### 4. Discussion

As shown in Fig. 1, the variations of $I_s$ with thermal hysteresis were entirely asymmetric. In connection with the experimental item (1) described in the last paragraph of Section 1, two kinds of crossover concentrations for random-coil chain and rod-like chain, $\phi_2^*$(coil) [45] and $\phi_2^*$(rod) [46], were calculated theoretically from the value of $M_w$ to be $2.3 \times 10^{-3}$ and $1.4 \times 10^{-5}$, respectively. Presumably, it is likely that the value of $\phi_2^*$ for the worm-like chain is intermediate between $\phi_2^*$(coil) and $\phi_2^*$(rod) [47].
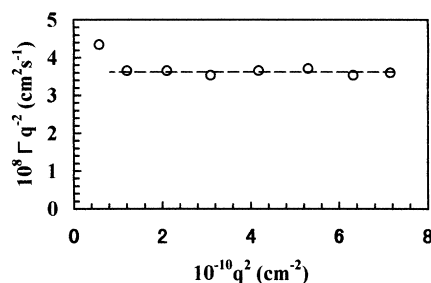


Fig. 7. Plots of $\Gamma q^{-2}$ versus $q^2$ in the yellow phase in the presence of Triton X-100. The broken line is the averaged value of $\Gamma q^{-2}$, which was determined in a similar manner as above (Fig. 4).
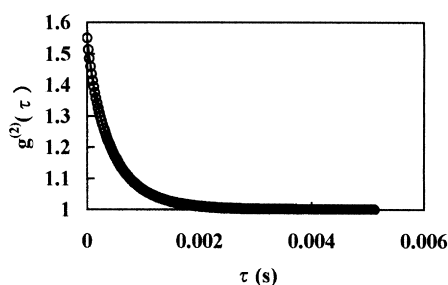
Fig. 8. Decay curve of $g^{(2)}(\tau)$ measured at $t_{323\ K} = 12$ (red phase). The full line represents the best fit by Eqs. (1) and (2). $\theta$ was 90°.

## 4.1. Yellow phase at 353 K

Wegner et al. have demonstrated that $R_h$ of poly(4BCMU) ($M_w = 1.67 \times 10^6$) in the CHCl$_3$ solution was 51 nm at room temperature (293 K) [34]. In addition, Chu et al. reported that $R_h$ for the same polymer with $M_w = 2.4 \times 10^6$ was 84 nm in CHCl$_3$ at room temperature [37]. These CHCl$_3$ solutions can be regarded as a good solvent state at room temperature, corresponding to toluene solution at the elevated temperature [20]. In fact, Heeger et al. estimated from the DLS measurements that $R_h$ of poly(4BCMU) ($M_w = 1.18 \times 10^6$) dissolved in toluene was ca. 40 nm in the yellow phase at 343 K [28].

According to the following worm-like chain model proposed by Hearst, Stockmeyer, and Yamakawa [47–49], $R_h$ can be evaluated theoretically to be ca. 45 nm on the assumptions that the contour length $L$ is 1000 nm (which corresponds to $M_w \cong 10^6$), the persistence length $P_L$ is 15 nm [34,37], the monomer length $M_L$ is 0.5 nm, and that the diameter of monomer $d$ is 6 nm in the case of a poly(4-BCMU) chain:

$$R_h = L[2\{1.843(L/2P_L)^{1/2} - \ln(M_L/2P_L) - 2.431$$

$$- (M_L/d)\}]^{-1} \text{ at } L/2P_L \gg 1 \qquad (5)$$

Compared with these earlier mentioned values, $R_h$ measured in the present work was strikingly much larger in the yellow phase, regardless of a dilute regime: $\phi_2 < \phi_2^*(\text{coil})$, and has scarcely been influenced by changing $\phi_2$ within a dilute region. In this connection, the second virial coefficients $A_2$, corresponding to the slopes in Fig. 5,
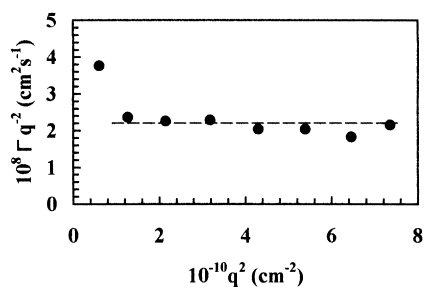


Fig. 9. Relationship between $\Gamma q^{-2}$ and $q^2$ at $t_{323\ K} = 12$ in the red phase. The broken line is the averaged value of $\Gamma q^{-2}$.

were negative, and $R_h$ decreased remarkably by adding the surfactants as listed in Table 1. However, it is likely that poly(4BCMU) chains were not isolated completely in the yellow phase, even if the surfactants were added. Moreover, the exponent $\gamma$ in Eq. (2) was nearly unity, which may imply usually mono-dispersed distribution of molecular weight [42], although poly(4BCMU) has a broad distribution of molecular weight as described in Section 2. These facts suggest that a certain cluster-like weak interaction may exist between poly(4BCMU) chains in the yellow phase. This experimental result is a hitherto unknown, at least, in CHCl$_3$ solutions [20] and in toluene solutions at 353 K below [28]. However, it is not so surprising to find the associates to be relatively mono-disperse, as in many colloidal systems [50].

Recently, the associative polymers with attractive functional groups were investigated in detail [51]. These polymers would form the interesting and important classes of polymeric systems: charged polymers (ionomers, polyelectrolytes, etc.), block copolymers in strong selective solvents, and polymers with hydrogen bondings. For example, it was reported that cellulose diacetate in dilute $N$, $N$-dimethylacetamide solutions indicated three kinds of the decay modes in the measured ACF [52]. The last two decay modes with longer correlation times were assigned to be a cluster of cellulose derivatives and a structure among the clusters associated through hydrogen bondings even in a dilute region, which size ($R_h$) was of order of μm. Such a cluster and an associated structure were likely to be non-equilibrium and unstable, because they could not be detected from the measurements of sedimentation coefficients with ultra-centrifuge methods [52].

In the present case, not only rotation-restricted stiff polymer backbone but also intra-molecular hydrogen bondings between urethane parts in side chains essentially play a important part in the retention of a worm-like conformation of a poly(4BCMU) chain [27,53]. The most probable reason may be speculated; that is, when the motion of a poly(4-BCMU) chain with worm-like conformation becomes thermally more flexible at the elevated temperature like 353 K, some intra-molecular hydrogen bondings would be broken partially, where weak interactions may be newly caused by generating intra-molecular hydrogen bondings [54]. Consequently, poly(4BCMU) chains would make it possible to form weakly interacted cluster-like domains. If poly(4-BCMU) may exist as an isolated chain at 353 K, the shape of the chain probably is still worm-like and non-spherical. This must lead to an optical anisotropy in light scattering measurements, obviously non-unity of the exponent $\gamma$ in Eq. (2), and to strong dependence of $\Gamma q^{-2}$ on $q^2$ [34,36]. No tendencies, however, have been observed in Fig. 4, except for the up-turn phenomenon in the low $q$-region. The intermolecular hydrogen bondings newly formed appear to be cut easily by adding surfactants. Anyway, it is important that a balance between disappearance of intra-molecular hydrogen bondings and formation of inter-molecular ones
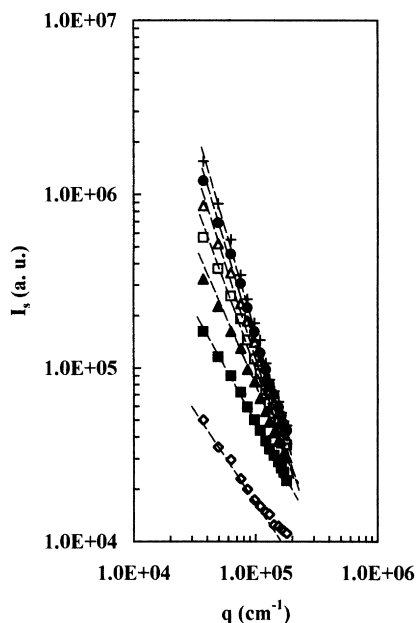
Fig. 10. Time ($t_{323\,K}$)-evolution of $I_s$ as a function of $\boldsymbol{q}$ in the red phase. The symbols represent in order $t_{323\,K} = 0$ (the bottom) to $t_{323\,K} = 13$ (the top) every 2 h.

should be established at an optimum elevated temperature [28]. The broad distribution of molecular weight of poly(4-BCMU) may be also affected by such association phenomenon in the yellow phase.

## 4.2. Red Phase at 323 K

The value of $R_h$ was 88 nm at $t_{323\,K} = 0$, and the $D$ value was roughly unity. The calculated values of $R_h$ could be, respectively, estimated to be 90 nm to 110 nm from the Kirkwood–Riseman's equation (6) [55] and the Schmidt's relation (7) [56] by assuming that poly(4BCMU) would be a single thin rod-like chain:

$$R_h = L[2\ln(L/d)]^{-1} \tag{6}$$

$$R_h = L[2\ln(L/d) - \delta]^{-1} \tag{7}$$

where, $\delta$ in Eq. (7) is a numerical value, being usually 1.1 to 1.5. The slight red-shift of $\lambda_{max}$ within the initial 2 h as shown in Fig. 11(c) may reflect that $\pi$-conjugated poly(4-BCMU) chains which were not locally extended fully along the backbone [57]. As a first approximation, however, the agreement in $R_h$ between calculated and measured values suggests that poly(4BCMU) may take the conformation like a single rod-like chain at $t_{323\,K} = 0$, which is also supported from the value of $D$ [44]. Actually, Abs($\lambda_{max} = 535$ nm) has already appeared at around 340 K (not shown). This fact implies that the poly(4BCMU) chain begins to be locally extended along a main chain, which may bring about the decomposition of the domains formed in the yellow phase.

The increases in $R_h$ and $D$ shown in Fig. 11(a) and (b) indicate evidently an aggregation process between rod-like
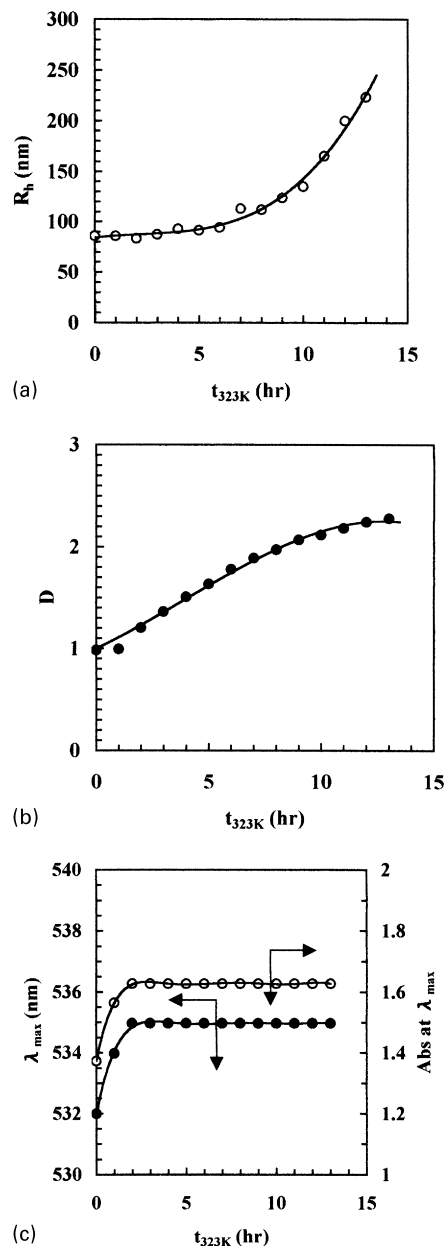


Fig. 11. (a) Variations of hydrodynamic radius $R_h$ with $t_{323\,K}$ in the red phase. The values of $R_h$ were determined by using Eq. (3); (b) Changes of fractal dimension $D$ with $t_{323\,K}$ in the red phase. The $D$ values were estimated from the following relation (see the text): $I_s \sim q^{-\alpha}$ as plotted in Fig. 10; and (c) Dependence of $\lambda_{max}$ and Abs($\lambda_{max}$) in visible absorption spectra with $t_{323\,K}$ in the red phase: $\lambda_{max}$, the wavelength at the maximum absorption peak; Abs($\lambda_{max}$), the absorbance at $\lambda_{max}$.

poly(4BCMU) chains. The number of aggregation ($NA$) estimated from the increment of $R_h$ was about 16 at $t_{323\,K} = 12$, which value was consistent approximately with those already reported by Chu ($NA = 14$) [58] or by Wegner ($NA = 30$) [34,37] in the same system (but at room temperature). Of course, it should be kept in mind that $NA$ is variable and delicately dependent on thermal hysteresis, solvent quality, etc. In addition, the saturated value of $D$ has remained less than three, which describes that the
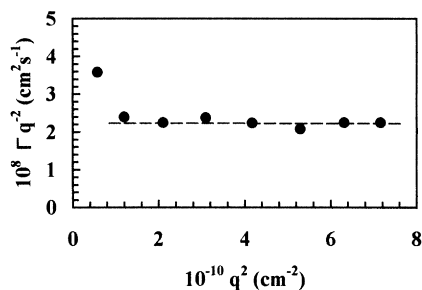
Fig. 12. Plots of $\Gamma q^{-2}$ versus $q^2$ at $t_{323\ K} = 12$ in the presence of Triton X-100. The broken line is the averaged value of $\Gamma q^{-2}$.

whole structure of aggregated poly(4BCMU) essentially referred to mass fractals [43,44]. In general, an increase in $D$ is equivalent to the compactness becoming dense in mass fractal structure [43,59]. In Fig. 11(a), $R_h$ nearly increased exponentially until $t_{323\ K} = 12$, rather than power-law kinetics [38]. There are theoretically two limited aggregation kinetics [43]. One is the fast aggregation as predicted by the diffusion-limited cluster aggregation (DLCA) model, in which $D$ is usually 1.75 to 1.8, and the other the slow aggregation represented by the reaction-limited cluster aggregation (RLCA) model with $D = 2.1$. Aggregated structures grow up with time according to power-law relation in the former case, while the exponential

kinetics is generally observed in the latter case as shown in Fig. 11(a) [60].

The aggregation would be anticipated to be promoted not only by a lowering of the solvent quality with decreasing temperature but also by an enlargement of the effective concentration, that is to say, the ratio of $\phi_2/\phi_2{}^*$(rod) was more than one hundred times higher than the $\phi_2/\phi_2{}^*$(coil) in calculation. In other words, poly(4BCMU)-toluene solution in the red phase was obviously near at the crossover concentration, where polymer chains are in contact with each other in a transient network structure [45]. Although the surfactants added have not affected the aggregation process in the red phase, it is well-known that trifluoroacetic acid or phenol can decompose an aggregated gel-like structure in concentrated poly(4BCMU) solution [61].

Consider further the problem for rod-like poly(4BCMU) aggregated in the red phase. Thus far, most studies on chromatic transition for soluble PDA solutions were performed in mixed solvents, consist of toluene and $CHCl_3$, at room temperature in any hypotheses of an intra-molecular and an inter-molecular effect [28–34,37,38,57,58]. Here, our attention should be focused on temperature and concentration. Poly(4BCMU) may aggregate easily in a poor solvent such as toluene at room temperature. It took more than a few days to be reached to the steady-state under certain circumstances [20]. The ranges of $\phi_2$ in the previous investigations
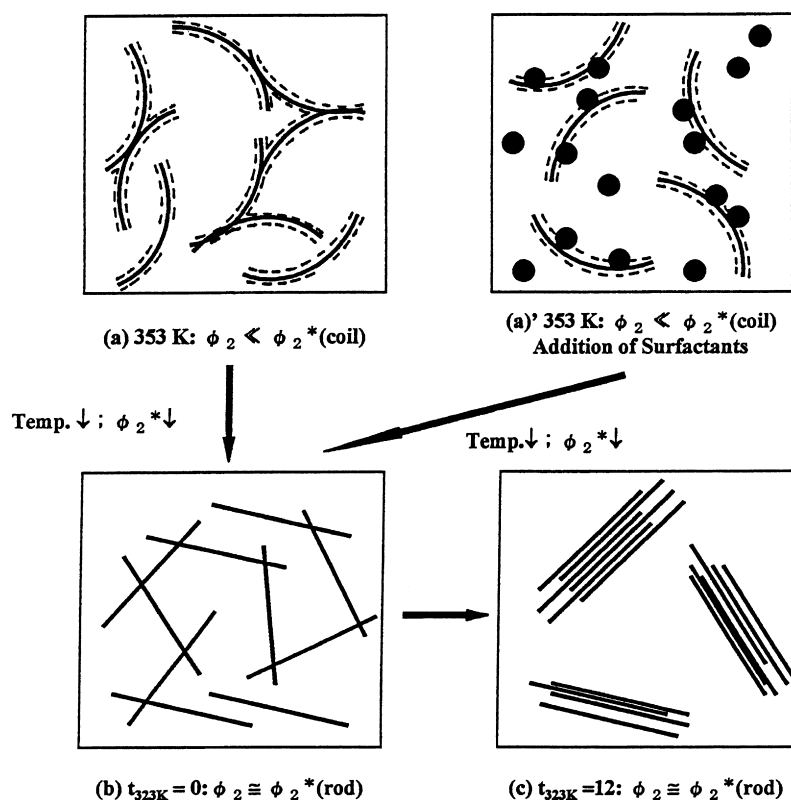


Fig. 13. Proposed scheme of chromatic transition and the subsequent aggregation for poly(4BCMU) in toluene solution. In (a) and (a)', the full and dotted lines represent polymer backbones and intra-molecular hydrogen bonds between urethane parts in side chains, respectively. The closed circles in (a)' illustrate the added surfactant. In (a), the intra-molecular hydrogen bondings are thermally broken partially, where inter-molecular hydrogen bondings are formed newly; (b) displays a single rod-like poly(4BCMU); and (c) is an aggregated state.

remained to be $10^{-5}$ to $10^{-6}$, which is just in the vicinity of $\phi_2^*$(rod). Actually, $\phi_2$ was also of the order of $10^{-5}$ in the present work. In general, a crossover concentration is not so critical and has a certain width, being influenced mainly by a distribution of molecular weight, shape of polymer chain, solvent quality and temperature [45]. To experimentally prevent an aggregation, one has to control carefully the conformation of poly(4BCMU) chain with high precision at room temperature, and need evaluate $R_h$ in an extremely diluted solution [20].

Heeger et al. have demonstrated that poly(4BCMU) ($M_w \cong 10^6$) chains may dissolve stably as an 'isolated' rod-like chain in toluene solution even at room temperature [28], irrespective of $\phi_2 < 10^{-5}$, and have proposed the intra-molecular rod-to-coil conformational transition of poly(4-BCMU) as described in Section 1. According to Heeger's suggestion, it was very important and difficult to obtain a 'good' sample solution prepared by filtering and handling carefully to avoid an aggregation [28]. Otherwise, the problem will appear to arise from a tendency toward aggregation. However, no more than detailed experimental procedures were described unfortunately for the purpose of preparing a 'good' sample solution [28].

Anyway, to understand well chromatic transition and the subsequent aggregation in the red phase, it would be emphasized in the present work that the temperature such as 323 K in the red phase was chosen as a moderate state of poor solvent in such a way that the time-resolved data could be obtained, instead of investigating in an extremely dilute solution [20].

## 5. Conclusions

Fig. 13 indicates the proposed scheme of chromatic transition and the subsequent aggregation for poly(4BCMU)-toluene system. In the yellow phase at 353 K, poly(4-BCMU) may make a weak interaction through inter-molecular hydrogen bondings formed newly at the break points of intra-molecular hydrogen bondings between urethane parts in side chains, resulting from thermal motion along a main chain with worm-like conformation. As a result, the weakly interacted cluster-like domains were produced consequently in the yellow phase, which would result in a large $R_h$. This interpretation could be supported mainly from the following experimental facts: negative $A_2$, the effects of added surfactants, and approximately the unity of the exponent $\gamma$ in Eq. (2).

On the other hand, by choosing the temperature of 323 K as a moderate state of poor solvent in the red phase, it has become first apparent from the variations of $R_h$ and $D$ with time that poly(4BCMU) might take initially a single rod-like conformation, and then the subsequent aggregation has proceeded gradually. Probably, this seems to be one of the possible answers for 'the chicken or the egg argument', which was stated by Chu [20]. No surfactants used have

affected the aggregation process. There are, however, still uncertainties in the influence of charged poly(4BCMU) chains, owing to $\gamma$-irradiation in the synthesis and long $\pi$-conjugation [20,62–64], to aggregation phenomena.

## References

[1] Cantow H-J, editor. Polydiacetylenes: Adv Polym Sci, vol. 63. Berlin: Springer, 1984.
[2] Tashiro K, Nishimura H, Kobayashi M. Macromolecules 1996;29:8188.
[3] Yang Y, Lee Y, Miller P, Li L, Kumura J, Tripathy S-K, Matsuda H, Okada S, Nakanishi H. Mater Res Soc Symp Proc 1991;214:177.
[4] Gason S-J, Dunstan D-E, Smith JA, Chan DYC, White LR, Boger DV. J Phys Chem 1997;101:7732.
[5] Palchetti L, Li Q, Giorgetti E, Grando D, Sottini S. Appl Opt 1997;36:1204.
[6] Hambir AA, Wolfe D, Blanchard GJ, Baker GL. J Am Chem Soc 1997;119:7367.
[7] Rochfold KB, Zanoni R, Gong Q, Stegeman GI. Appl Phys Lett 1989;55:1161.
[8] Paley MS, Frazier DO, Abdeldeyem H, Armstrong S, McManus SP. J Am Chem Soc 1995;117:4775.
[9] Bredas JL, Silbey R. The novel science and technology of high conducting and nonlinear optically active materials, Dordrecht. The Netherlands: Kluwer Academic Publishers, 1991.
[10] Wong KS, Han SG, Vardeny ZV. Synth Met 1991;41:3209.
[11] Bogler J, Harvey TG, Ji W, Kar AK, Molyneux S, Wherrett BS, Bloor D, Neerman P. J Opt Soc Am 1992;B9:1552.
[12] Hsu CC, Kawabe Y, Ho ZZ, Peyghambarain N, Polky JN, Krung W, Miao E. J Appl Phys 1990;67:7199.
[13] Korshak YV, Medvedeva TV, Ovehinnikov AA, Spektov VN. Nature 1987;326:370.
[14] Shutt JD, Rickert SE. Langumuir 1987;3:460.
[15] Garito AF, Shi RF, Wu MH. Physical Today 1994;47:51.
[16] Helfin JR, Garito AF. Third-order nonlinear optical processes in linear chain. In: Hornah LA, editor. Polymers for lightwave and integrated optics. New York: Marcel Dekker, 1992.
[17] Nalwa HS. Organic materials for third-order optical nonlinearities. In: Nalwa HS, Miyata S, editors. Nonlinear optics of organic molecules and polymers, chap. 10. New York: CRC Press Inc., 1997.
[18] Baugham RH, Chance RR. J Polym Sci Polym Phys Ed 1976;14:2037.
[19] Kodai NB, Kim W, Kumar J, Tripathy SK. Macromolecules 1994;27:6612.
[20] Chu B, Xu R. Acc Chem Res 1991;24:384.
[21] Lim KC, Fincher CR, Heeger AJ. Phys Rev Lett 1934;1983:50.
[22] Berlinsky AJ, Wudl F, Lim KC, Fincher CR, Heeger AJ. J Polym Sci Polym Phys Ed 1984;22:847.
[23] Chance RR, Sowa JM, Eckhardt H, Schlott M. J Phys Chem 1986;90:3031.
[24] Chen P, Adachi K, Kotaka T. Polym J 1993;25:473.
[25] Prusik T, Montesalvo M, Wallance T. Radiat Phys Chem 1988;31:441.
[26] Variano BF, Sandroff CJ, Baker GL. Macromolecules 1991;24:4376.
[27] Patel GN, Chance RR, Witt JD. J Chem Phys 1979;70:4387.
[28] Lim KC, Heeger AJ. J Chem Phys 1985;82:522.
[29] Lim KC, Kapitulnik A, Zacher R, Heeger AJ. J Chem Phys 1985;82:516.
[30] Lim KC, Kapitulnik A, Zacher R, Heeger AJ. J Chem Phys 1986;84:1058.
[31] Wenz G, Muller MA, Schmidt M, Wegner G. Macromolecules 1984;17:837.
[32] Muller MA, Schmidt M, Wegner G. Makromol Chem Rapid Commun 1984;5:83.

[33] Schmidt M, Wegner G. J Chem Phys 1986;84:1057.

[34] Rawiso M, Aime JP, Fare JL, Scott M, Muller MA, Schmidt M, Baumgartl H, Wegner G. J Phys France 1988;49:861.

[35] Brown W. Light scattering, principles and development. Oxford: Oxford Science Publishers, 1996.

[36] Brown W. Dynamic light scattering, the method and some applications. Oxford: Oxford Science Publishers, 1993.

[37] Xu R, Chu B. Macromolecules 1989;22:3153.

[38] Li Y, Chu B. Macromolecules 1991;24:4115.

[39] Kohlrausch R. Ann Phys (Leipzig) 1847;12:393.

[40] Williams G, Watts DC. Trans Faraday Soc 1970;66:80.

[41] Pecora R. J Chem Phys 1965;43:1562.

[42] Pecrora R. Dynamic light scattering. New York: Plenum Press, 1985.

[43] Avnir D. The fractal approach to heterogeneous chemistry. New York: Wiley, 1989.

[44] Schmidt PW. J Appl Cryst 1991;24:414.

[45] De Gennes PG. Scaling concept in polymer physics. Ithaca, New York: Cornell University Press, 1979.

[46] Doi M, Edward SF. J Chem Soc Faraday Trans 2 1978;74:560, 918.

[47] Yamakawa H. Modern theory of polymer solutions, New York: Harper and Row Publishers, 1971.

[48] Hearst JE, Stockmayer WH. J Chem Phys 1962;37:1425.

[49] Hearst JE. J Chem Phys 1963;38:1062.

[50] Lee KW. J Colloid Interface Sci 1983;92:315.

[51] Rubinstein M, Dobrynin AV. Trend Polym Sci 1997;5:181.

[52] Kawanishi H, Tsunashima Y, Horii F. Polym Prep Jpn 1996;45:754.

[53] Nava AD, Thakur M, Tonelli AE. Macromolecules 1990;23:3055.

[54] Joesten MD, Schaad LJ. Hydrogen bondings. New York: Dekker, 1974.

[55] Rieseman J, Kirkwood JG. J Chem Phys 1950;18:512.

[56] Schmidt M. Macromolecules 1984;17:553.

[57] Peiffer DG, Chung TC, Schulz DN, Agarwal PK, Garner RT, Kim MW. J Chem Phys 1986;85:4712.

[58] Chu B, Xu R, Li Y, Wu DQ. Macromolecules 1989;22:3819.

[59] Dadmun MD, Muthukumar M, Schwahn D, Springer T. Macromolecules 1996;29:207.

[60] Zhou Z, Chu B. J Colloid Interface Sci 1991;143:356.

[61] Chen P, Adachi K, Kotaka T. Polymer 1993;34:4953.

[62] Xu R, Chu B. Macromolecules 1989;22:4523.

[63] Coehn A, Raydt V. Ann Phys (Leipzig) 1909;30:777.

[64] Zacher RA. J Chem Phys 1990;93:1325, 2139.